JACS
JOURNAL OF THE AMERICAN CHEMICAL SOCIETY

Subscriber access provided by American Chemical Society

Article

Mixed 1D–2D Inorganic Polymeric Zinc Ferrocenylphosphonate: Crystal Structure and Electrochemical Study

Olivier Oms, Jean Le Bideau, Fabrice Leroux, Arie van der Lee, Dominique Leclercq, and Andr Vioux

J. Am. Chem. Soc., **2004**, 126 (38), 12090-12096• DOI: 10.1021/ja049457p • Publication Date (Web): 04 September 2004

Downloaded from http://pubs.acs.org on April 1, 2009

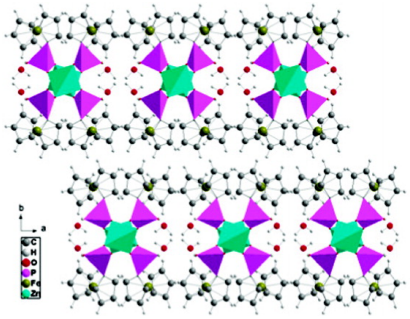

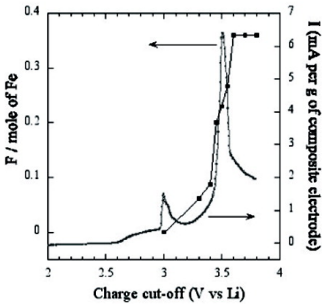

More About This Article

Additional resources and features associated with this article are available within the HTML version:

- Supporting Information
- Links to the 2 articles that cite this article, as of the time of this article download
- Access to high resolution figures
- Links to articles and content related to this article
- Copyright permission to reproduce figures and/or text from this article

View the Full Text HTML

ACS Publications
High quality. High impact.

Journal of the American Chemical Society is published by the American Chemical Society. 1155 Sixteenth Street N.W., Washington, DC 20036

J|A|C|S
ARTICLES
Published on Web 09/04/2004

Mixed 1D−2D Inorganic Polymeric Zinc Ferrocenylphosphonate: Crystal Structure and Electrochemical Study

Olivier Oms,[†] Jean Le Bideau*,[†] Fabrice Leroux,[‡] Arie van der Lee,[§] Dominique Leclercq,*,[†] and André Vioux[†]

Contribution from the Laboratoire de Chimie Moléculaire et Organisation du Solide, UMR 5637, Université Montpellier II, CC 007, Place Eugène Bataillon, 34095 Montpellier Cedex 05, France, Laboratoire des Matériaux Inorganiques, UMR 6002, Université Blaise Pascal, 63177 Aubière Cedex, France, and Institut Européen des Membranes, UMR 5635, Université Montpellier II, CC 047 Place Eugène Bataillon, 34095 Montpellier Cedex 05, France

Received January 30, 2004; E-mail: lebideau@univ-montp2.fr

Abstract: Needs for ferrocene immobilization on robust host structures are considerable since derivative materials may find applications in medical areas, optical devices, or catalysis. Synthesis of phosphonate functionalized ferrocene allowed its subsequent inorganic polymerization with a zinc salt. The crystallographic structure of the compound obtained, $Zn(HO_3PFc)_2{\cdot}2H_2O$, shows a unique two-dimensional ferrocene arrangement anchored on a one-dimensional Zn−O−P−O−Zn backbone. The ferrocene packing in the title compound is very similar to the packing found in molecular ferrocene. The electroactivity of $Zn(HO_3PFc)_2{\cdot}2H_2O$ is thoroughly studied. It shows a reversible surface oxidation of ferrocene. Mössbauer spectroscopy for the oxidized compound shows an isomer shift of $IS_{2b} = 0.432$ mm.s^{-1} and a quadrupolar splitting of $QS_{2b} = 0.205$ mm.s^{-1}, which is consistent with a stable S = 1/2 ferrocenium state. The magnetic susceptibility study, Mössbauer spectroscopy, and galvanostatic titration show that only the ferrocene moieties present at the surface of the crystallites are reversibly oxidized. This observation is reinforced by a complex impedance study showing mainly resistive behavior and conductivity measurements indicating weak, thermally assisted, conductivity. The general properties of this compound demonstrate that phosphonato functionalization may be a useful approach for all fields concerned by immobilization of ferrocene.

Introduction

The desire to design materials by molecular assembly increases dramatically as research continues to improve the correlation between the resulting devices and molecular properties. Crystal engineering aims at rationalizing chemical synthesis for targeted purposes rather than using the criticized "shake and bake" method. The expansion of the field of crystal engineering along with the increase of hybrid organic−inorganic materials research has necessitated a classification of the types of resulting compounds. On one hand, the engineering of coordination polymers[1] excludes compounds in which no carbon atom is present as bridging ligand; on the other hand, the reticular synthesis[2] requires the use of predesigned building blocks. However, both cases involve the connection of metal cations by means of hybrid building blocks such as carboxylates or amines. Our approach is based on phosphonate ligands, use of which has shown a great expansion in the last 20 years.[3,4] The first step in this approach is to chemically functionalize the chosen molecule by a phosphonato group. The resulting rigid building block retains its structural integrity during the subsequent steps of the material construction.

Prompted by the current efforts on functional polymeric materials bearing ferrocene groups,[5−7] we have synthesized the ferrocenylphosphonic acid subsequently used for inorganic polymerization with metal salts, thus yielding a material having ferrocene properties in association with a robust inorganic backbone.

Ferrocene derivatives are of considerable interest in many areas.[8,9] Asymmetric catalysis activity of metallocenes was shown to be efficient by their immobilization in a robust host structure.[10] Immobilization of ferrocene has opened applications

[†] CMOS, Université Montpellier II.
[‡] LMI, Université Blaise Pascal.
[§] IEM, Université Montpellier II.

(1) Janiak, C. *Dalton Trans.* **2003**, 2781−2804.
(2) Yaghi, O. M.; O'Keeffe, M.; Ockwig, N. W.; Chae, H. K.; Eddaoudi, M.; Kim, J. *Nature* **2003**, *423*, 705−714.
(3) Clearfield, A. In *Progress in Inorganic Chemistry*; Karlin, K. D., Ed; John Wiley & Sons: New York, 1998; Vol. 47, pp 371−510.
(4) Vioux, A.; Le Bideau, J.; Mutin, P. H.; Leclercq, D. In *Topics in Current Chemistry*; Majoral, J.-P., Ed.; Springer-Verlag: Heidelberg, Germany, 2004; Vol. 232, pp 145−174.
(5) Kulbaba, K.; Manners, I. *Macromol. Rapid Commun.* **2001**, *22*, 711−724.
(6) Hudson, R. D. A. *J. Organomet. Chem.* **2001**, *637−639*, 47−69.
(7) Rehahn, M. *Mater. Sci. Technol.* **1999**, *20*, 319−374.
(8) *Metallocenes*; Togni, A., Haltermann, R. L., Eds.; Wiley-VCH: New York, 1998.
(9) *Ferrocenes: Homogeneous Catalysis, Organic Synthesis, Materials Science*; Togni, A., Hayashi, T., Eds.; VCH Publishers: New York, 1995.
(10) Colacot, T. J. *Chem. Rev.* **2003**, *103*, 3101−3118.

10.1021/ja049457p CCC: $27.50 **© 2004 American Chemical Society**

in photochromic devices,[11] nonlinear optics,[12,13] neutral molecules sensing and gas sensing,[14−16]cations sensing,[17,18] glucose sensors,[19−23] biosensing of hybridization of DNA,[24−27] antibodies diagnostic tests,[28] and antiproliferative chemotherapeutic agent in cancer research.[29,30] For antitumor activity, platinum ferrocenyl-phosphonate complexes were studied, of which ferrocenylphosphonic acids precursors were reported in the literature.[31]

Phosphonates have shown interesting immobilization potential on metal oxides because of the high stability of M−O−P bonds toward hydrolysis.[4] During our investigations on phosphonates, we aimed at preparing metal oxide−ferrocenyl phosphonate networks. We present in this paper a zinc bis(ferrocenylphosphonate) $Zn(HO_3PFc)_2{\cdot}2H_2O$ were Fc stands for (C_5H_4)-$Fe(C_5H_5)$, for which the synthesis of the ferrocenylphosphonic acid was first required. The limitation of reports in the literature on metal ferrocenylphosphonates may be attributed to the low yield reported for the synthesis of ferrocenylphosphonic acid.[31] A large improvement of this yield has been achieved by using the *t*-BuLi/*t*-BuOK system at low temperature to form the monolithioferrocene. The increase of the yield from 24 to 67% allows its use as a building block for electroactive metal phosphonate materials.[32] The hybrid compound $Zn(HO_3PFc)_2{\cdot}2H_2O$ resulting from this improved synthesis pathway displayed a very original single crystal structure showing simultaneously 1D and 2D structural features. Ion transport properties are studied by complex impedance spectroscopy. Fe Mössbauer spectroscopy completes the characterization of the oxidation state of iron cations undergoing an oxidation reaction. Finally, the level of iron cations which can be oxidized is evaluated by electrochemical measurements and correlated with Mössbauer and magnetic properties studies.

Results

Crystal Structure. The compound crystallizes in the orthorhombic system in space group *Pccn*. Table 1 summarizes the crystallographic data for the zinc bis(ferrocenylphosphonate).

Table 1. Crystallographic Data; (1) for All Reflections; (2) for Reflections $I > 2\sigma(I)$

formula	$Zn_{0.5}FePO_4C_{10}H_{12}$
formula weight	315.71
crystal system	orthorhombic
space group	Pccn
a/Å	9.6950(10)
b/Å	26.700(3)
c/Å	8.8640(10)
V/Å^3	2294.5(4)
Z	8
D/g.cm^{-3}	1.828
λ/Å	0.71073
μ/cm^{-1}	2.469
T/K	173
2θ min/max	3.0/32.4
total no. of indep. reflcns	3817
total no. reflcns $I > 2\sigma(I)$	736
no. of variables	80
R_F2 (1)	0.1969
R_F2 (2)	0.0625
wR_F2 (1)	0.0385
wR_F2 (2)	0.0419
res. density min/max	−0.57/0.65
GOF	1.13

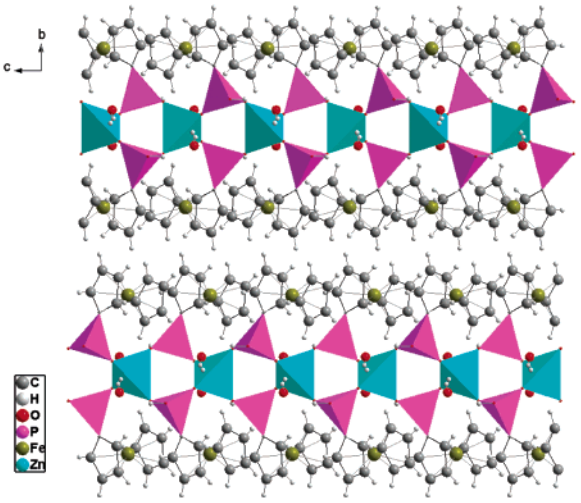

Figure 1. $Zn(HO_3PFc)_2{\cdot}2H_2O$ viewed down the *a* axis, showing the Zn−O−P−O−Zn chains; Zn atoms are located at the center of blue tetrahedrons and P atoms at the center of pink tetrahedrons; O atoms of the water molecule are presented as red circles.

The crystallographic structure consists of Zn−O−P−O−Zn chains arranged as sheets which are separated by ferrocene double layers. The chains are formed by Zn−O tetrahedrons, of which each is connected to two neighboring Zn−O tetrahedrons through two phosphonato bridges forming the chains along the *c* axis (Figure 1).

Within each sheet of chains, the chains are separated by channels occupied by the water molecules (Figure 2).

Two phosphonato oxygen atoms are thus linked to two neighboring zinc atoms and on the third oxygen atom (O6) remains a hydrogen atom (H27). The structure suggests that this hydrogen atom is hydrogen-bonded with a water molecule placed between two neighboring chains (O17) (Figure 3). This interaction is at 1.55 Å, too short for classical hydrogen bonding. Actually, the hydrogen atoms of the hydroxyl group and the water molecule were hardly visible in the Fourier difference map, so that they are not too well placed with respect to their

(11) Yokoyama, Y. *Yukagaku* **2002**, *33*, 226−228.
(12) Krishnan, A.; Pal, S. K.; Nandakumar, P.; Samuelson, A. G.; Das, P. K. *Chem. Phys.* **2001**, *265*, 313−322.
(13) Calabrese, J. C.; Cheng, L. T.; Green, J. C.; Marder, S. R.; Tam, W. *J. Am. Chem. Soc.* **1991**, *113*, 7227−7232.
(14) Bucher, C.; Devillers, C. H.; Moutet, J.-C.; Royal, G.; Saint-Aman, E. *Chem. Commun.* **2003**, 888−889.
(15) Kim, C.; Park, E.; Song, C. K.; Koo, B. W. *Synth. Met.* **2001**, *123*, 493−496.
(16) Refaei, M.; Espada, L. I.; Shadaram, M. *Proc. of SPIE-Int. Soc. Opt. Eng.* **2000**, *4036*, 123−131.
(17) Pandey, P. C.; Upadhyay, S.; Pathak, H. C.; Pandey, C. M. D. *Electroanalysis* **1999**, *11*, 950−956.
(18) Ion, A.; Ion, I.; Moutet, J. C.; Pailleret, A.; Popescu, A.; Saint-Aman, E.; Ungureanu, E.; Siebert, E.; Ziessel, R. *Sens. Actuators, B* **1999**, *B59*, 118−122.
(19) Coche-Guerente, L.; Desprez, V.; Labbe, P. *J. Electroanal. Chem.* **1998**, *458*, 73−86.
(20) Foulds, N. C.; Lowe, C. R. *Anal. Chem.* **1988**, *60*, 2473−2478.
(21) Mizutani, F.; Asai, M. *Bull. Chem. Soc. Jpn.* **1988**, *61*, 4458−4460.
(22) Patel, H.; Li, X.; Karan, H. I. *Biosens. Bioelectron.* **2003**, *18*, 1073−1076.
(23) Pandey, P. C.; Upadhyay, S. *Sens. Actuators, B* **2001**, *B76*, 193−198.
(24) Korri-Youssoufi, H.; Makrouf, B. *Synth. Met.* **2001**, *119*, 265−266.
(25) Takagi, M. *Pure Appl. Chem.* **2001**, *73*, 1573−1577.
(26) Takenaka, S. Patent Jpn. 2000125865, 2000.
(27) Yu, C. J.; Wan, Y.; Yowanto, H.; Li, J.; Tao, C.; James, M. D.; Tan, C. L.; Blackburn, G. F.; Meade, T. J. *J. Am. Chem. Soc.* **2001**, *123*, 11155−11161.
(28) Yasuzawa, M.; Hamada, H.; Oga, K.; Mitsui, H.; Kunugi, A. *Proc.-Electrochem. Soc.* **2001**, *2001−18*, 653−656.
(29) Neuse, E. W. *Macromol. Symp.* **2001**, *172*, 127−138.
(30) Henderson, W.; Alley, S. R. *Inorg. Chim. Acta* **2001**, *322*, 106−112.
(31) Alley, S. R.; Henderson, W. *J. Organomet. Chem.* **2001**, *637−639*, 216−229.
(32) Oms, O.; Maurel, F.; Carré, F.; Le Bideau, J.; Vioux, A.; Leclercq, D. *J. Organomet. Chem.* **2004**, *689*, 2654−2661.

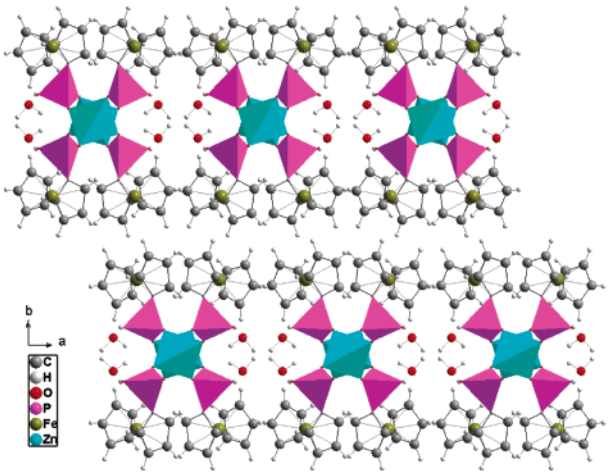

Figure 2. $Zn(HO_3PFc)_2 \cdot 2H_2O$ viewed down the *c* axis.

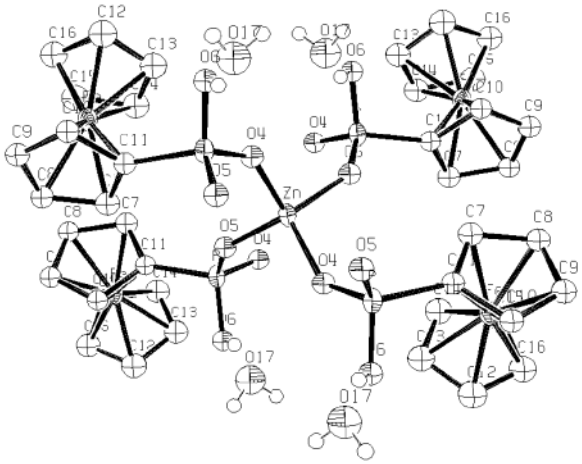

Figure 3. ORTEP view of the environment of Zn atom; H atoms on ferrocene have been omitted for clarity; H27 linked to O6 (POH) presents hydrogen bond with O17 (H_2O).

Table 2. Selected Bond Distances and Angles

distances/Å		angles/°	
Zn $O4^i$	1.939(6)	$O4^iZn\ O5^i$	109.6(3)
Zn $O5^i$	1.937(6)	$O5^iZn\ O5^{ii}$	117.0(4)
P $O4^i$	1.525(6)	$O4^iZn\ O5^{ii}$	104.1(3)
P O5	1.496(7)	$O4^iZn\ O4^{ii}$	112.7(4)
P O6 (POH)	1.567(7)	Zn $O4^iP$	140.6(4)
O6 H27 (POH)	1.114	Zn $O5^iP$	142.3(4)
P C1	1.765(6)	$O4^iP$ O6	107.1(4)
Fe C	2.02···2.05	$O4^iP$ C11	110.9(4)
C C	1.38···1.46	$O5^iP$ C11	108.3(4)
		P O6 H27	99.91
i: $-x + 1/2, y, z + 1/2$		P C11 C7	128.1(7)
ii: $x, -y + 1/2, z + 1/2$		P C11 C10	123.8(7)

parent atoms, and the presence of more peaks around the water molecule indicates that there is orientational disorder. The O6−H27 distance is a little bit too long (1.11 Å cf. expected ca. 0.8 Å, see Table 2), thus maybe explaining the short H27−O17 hydrogen bond obtained. It was not possible to improve the localization of these atoms since the quality of the data were limited by the very small size of the crystal (0.05-mm thick). Nevertheless, the hydroxyl group of the phosphorus environment pointed directly in the direction of the water oxygen atom.

The fourth corner of the phosphonato tetrahedron is occupied by a carbon atom coming from the ferrocene moiety. All local coordination distances are normal.

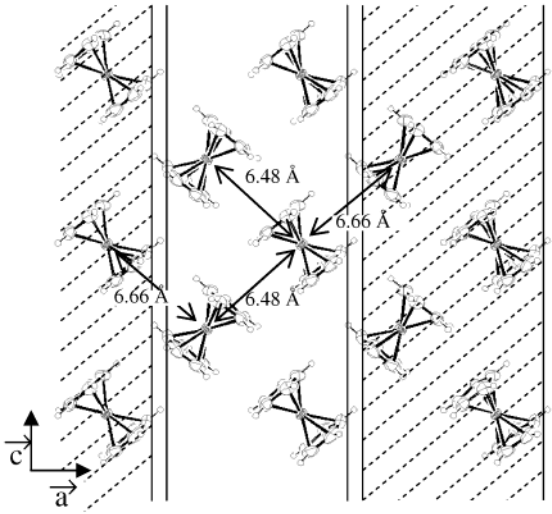

Figure 4. View down *b* of $Zn(HO_3PFc)_2 \cdot 2H_2O$; all atoms but one ferrocene layer have been omitted; nonshaded area represents ferrocene moieties linked to a single chain; shaded area ferrocene groups linked to a neighboring chain.

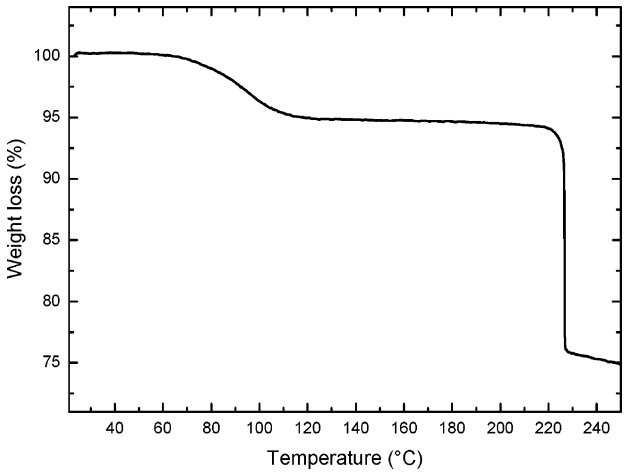

Figure 5. TGA: 2°C/mn, N_2 atmosphere.

More interesting is the arrangement of ferrocene moieties. They are arranged as layers, within which ferrocene groups are packed edge to face (Figure 4). Within a layer, the distance between two iron atoms from two neighboring ferrocene groups which are linked to the same chain is 6.48 Å, whereas the distance between two iron atoms from two neighboring ferrocene groups which are linked to two neighboring chains is 6.66 Å. The stacking of two ferrocene layers leads to the shortest Fe−Fe distance found in this compound at 5.67 Å. The cyclopentadienyl planes from the ferrocene moiety are nearly parallel (2.0°) and the conformation nearly eclipsed (1.3° rotation).

Thermal Behavior. Thermogravimetric analysis shows a pronounced weight loss around 85 °C, which is consistent with the departure of two water molecules. Further heating leads to the degradation of the compound, as shown by an important weight loss at 225 °C, which is consistent with the elimination of the nonsubstituted Cp rings (Figure 5).

At 90 °C, the thermodiffractogram of the title compound shows the disappearance of most of the diffraction lines except the first one. The first diffraction peak which was indexed (020)

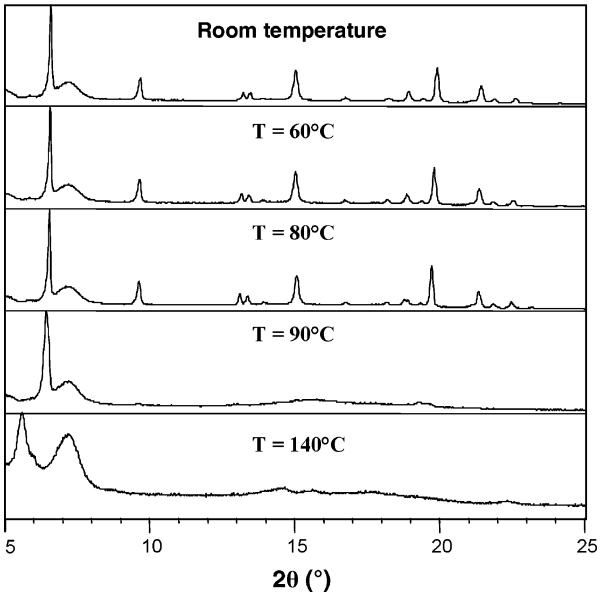

Figure 6. Thermodiffractograms; air, 4h/pattern.

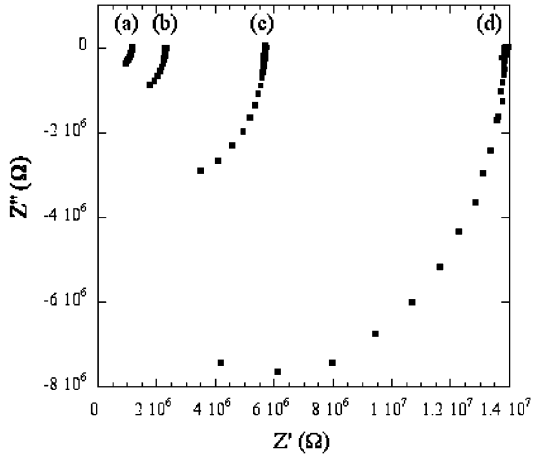

Figure 7. Complex impedance spectra recorded at (a) 354, (b) 338, (c) 319, and (d) 302 K.

presents a shift toward lower angle when the temperature increases. (Figure 6)

The broad signal at 7°2θ, the relative intensity of which increases upon heating, is due to the sample holder. The general evolution shows that the packing of the layers is retained after the loss of the water molecules, although the crystallographic order is lost between and within the Zn−O−P−O−Zn chains. The small increase in the distance between ferrocene double layers cannot be further explained because of the lack of structural information of the resulting compound.

Conductivity and Battery Study. The conductivity of the material was studied as a function of temperature between −20 and 80 °C. Typical impedance plots (Cole−Cole plot) are shown for four temperatures in Figure 7.

Impedance spectra consist usually of an arc in the high-frequency domain and a line inclined at 45° with respect to the *Z* axis in the low-frequency range. The straight line is explained by the ion blocking effect (modelized by RQ in the circuit), and the semicircle is affected mostly by the motion of the ions through and between particle boundaries (RK in parallel). The elements K and Q correspond to dielectric relaxation and electrode phenomena, respectively. The straight line in the low-frequency domain is not observed. The behavior is merely resistive even in the low-frequency domain.[33]

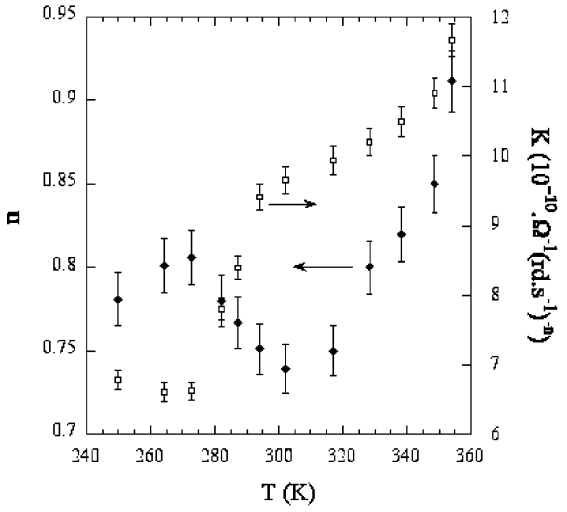

Figure 8. Variation of n and K in $Z_K = K^{-1}(j\omega)^{-n}$ as a function of temperature.

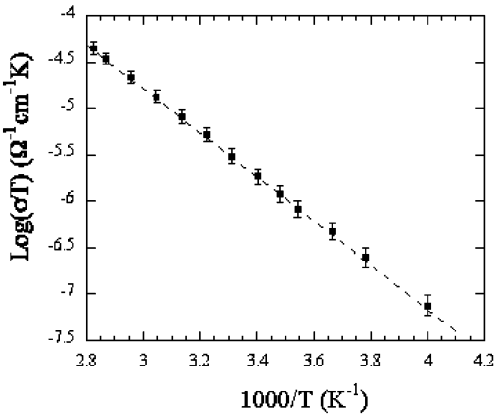

Figure 9. Arrhenius-type plot for $Zn(HO_3PFc)_2 \cdot 2H_2O$.

The values obtained after the refinements of the impedance spectra are displayed in Figure 8.

The capacitive value *K* obtained from the refined diameter of the high-frequency domain is about a few nF indicating that the grain-boundary response is predominant.[34,35] An increase in capacitance is observed as a function of temperature; this is also associated to a capacitive behavior becoming more and more ideal, $n \rightarrow 1$.

All the conductivity data were fitted to the Arrhenius expression $\sigma = \sigma_0 \exp(-E_a/kT)$, where σ_0 is a preexponential factor, E_a the activation energy, and k the Boltzmann constant. It can be observed that the data follow an Arrhenius law over the entire temperature range (Figure 9). This indicates that the process is thermally assisted, although the conductivity of the sample is weak.

To know whether the ferrocene moieties initially present in the sample may be oxidized, two electrochemical methods were employed. First, the response of the material was recorded under potentiostatic conditions. In the voltage domain 2−3.8 V versus

(33) Bianchi, D.; Casciola, M. *Solid State Ionics* **1985**, *17*, 7−12.
(34) Sanz, F.; Parada, C.; Rojo, J. M.; Ruiz-Valero, C. *Chem. Mater.* **1999**, *11*, 2673−2679.
(35) Amarilla, J. M.; Rojas, R. M.; Rojo, J. M.; Cubillo, M. J.; Linares, A.; Acosta, J. L. *Solid State Ionics* **2000**, *127*, 133−139.

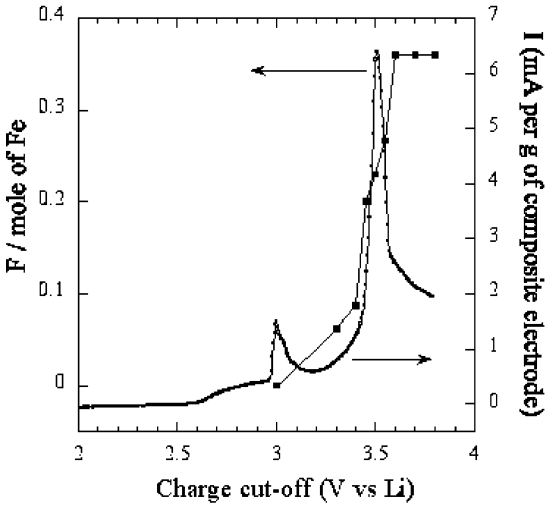

Figure 10. Electrochemical titration of the sample by potentiostatic (gray line) or galvanostatic (black square) method.

Li and during the anodic sweep, two peaks are observed: the first is irreversible, the second may be attributed to the response of the material (Figure 10). To support this hypothesis, a galvanostatic titration was then performed. During cycling, the discharge capacity was reported as a function of the voltage cutoff, V_C, at the end of the oxidation. By increasing progressively V_C, it is possible to recover a maximum of 0.35 electrons per mole of ferrocene in the subsequent discharge processes. We surmise that this value is due to the reversible oxidation of ferrocene to ferrocenium, the irreversible reaction that occurs during the charge process being discriminated by this technique. As a matter of fact, when V_C is increased to values higher than 3.6 V versus Li, there is no additional response in discharge whereas large irreversible capacities are obtained in charging.

Oxidation by Iodine. As it was impossible to recover the oxidized sample after the battery testing, another route of oxidation was tried. The oxidation of ferrocene by elementary iodine represents one of the most convenient procedures for the preparation of ferrocenium salts, the halogen acting both as the oxidant and as the anion source.[36] Exposure of the compound to iodine led to a sample **2** which was studied by IR and Mössbauer spectroscopy as well as by magnetic measurements. IR spectrum of **2** revealed a new vibration at 410 cm^{-1}, as expected for the antisymmetric ring metal stretching in ferrocenium;[37] the same vibration mode was found at 483 cm^{-1} for the title compound before oxidation. The Mössbauer spectra observed before and after oxidation by iodine are shown in Figure 11. Spectrum of initial $Zn(HO_3PFc)_2{\cdot}2H_2O$ **1** shows one doublet with an isomer chemical shift of $IS_1 = 0.431$ $mm.s^{-1}$ and a quadrupolar splitting of $QS_1 = 2.321$ $mm.s^{-1}$ with a relatively narrow line width of $\Gamma_1 = 0.230$ $mm.s^{-1}$. The difference of intensities between the two lines is commonly observed for samples presenting preferred orientation, which is the case here in view of the needle shape of the title compound, thus showing an anisotropic recoil-free fraction.[38] The oxidized compound **2** exhibits a Mössbauer spectrum with two doublets. The first one ($IS_{2a} = 0.428$ $mm.s^{-1}$, $QS_{2a} = 2.291$ $mm.s^{-1}$, $\Gamma_{2a} = 0.272$ $mm.s^{-1}$) corresponds to a nonoxidized part of the compound, and the second one ($IS_{2b} = 0.432$ $mm.s^{-1}$, $QS_{2b} = 0.205$ $mm.s^{-1}$, $\Gamma_{2b} = 0.272$ $mm.s^{-1}$) is characteristic of the S = 1/2 ground doublet of low-spin ferrocenium.[39−43] From the fitted signals, the amount of ferrocenium is 22.8(3.6)% of the initial ferrocene content. The molar magnetic susceptibility for compound **2** obeys a Curie−Weiss law with some temperature-independent paramagnetism contribution, that is, $\chi = C/(T - \theta) + \text{TIP}$ where $C = 0.268(1)$ $emu.K.mol^{-1}$, $\theta = -1.83(2)$ K, and TIP = 0.00363(2) $emu.mol^{-1}$. The TIP value is of the order of magnitude expected for such a contribution because of the availability of low-lying excited states.[44,45] A small negative θ value suggests some small antiferromagnetic interaction between paramagnetic centers.

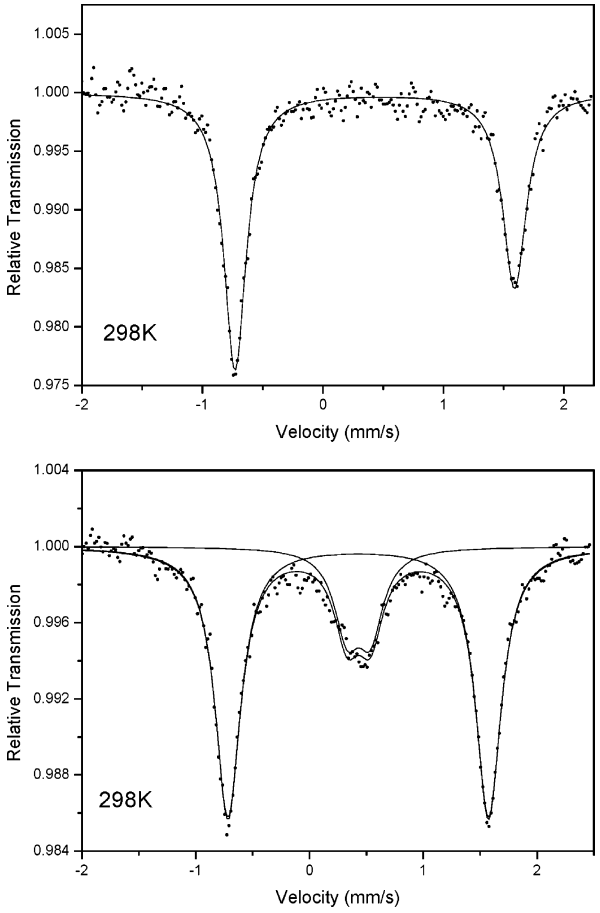

Figure 11. Mössbauer spectra for $Zn(HO_3PFc)_2{\cdot}2H_2O$ before (top) and after (bottom) chemical oxidation.

Discussion

The packing of the ferrocene molecules in the double layers in our zinc bis(ferrocenylphosphonate) is identical to the packing

(36) Neuse, E. W.; Loonat, M. S. *J. Organomet. Chem.* **1985**, *286*, 329−341.
(37) Pavlik, I.; Klikorka, J. *Collect. Czech. Chem. Commun.* **1965**, *30*, 664−674.
(38) Herber, R. H.; Nowik, I. *Solid State Sciences* **2002**, *4*, 691−694.
(39) Nagayoshi, K.; Khayrul Kabir, M.; Tobita, H.; Honda, K.; Kawahara, M.; Katada, M.; Adachi, K.; Nishikawa, H.; Ikemoto, I.; Kumagai, H.; Hosokoshi, Y.; Inoue, K.; Kitagawa, S.; Kawata, S. *J. Am. Chem. Soc.* **2003**, *125*, 221−232.
(40) Davidson, A.; Villeneuve, G.; Fournes, L.; Smith, H. *Mater. Res. Bull.* **1992**, *27*, 357−366.
(41) Miller, J. S.; Ward, M. D.; Zhang, J. H.; Reiff, W. M. *Inorg. Chem.* **1990**, *29*, 4063−4072.
(42) Miller, J. S.; Calabrese, J. C.; Rommelmann, H.; Chittipeddi, S. R.; Zhang, J. H.; Reiff, W. M.; Epstein, A. J. *J. Am. Chem. Soc.* **1987**, *109*, 769−781.
(43) Hendrickson, D. N.; Sohn, Y. S.; Gray, H. B. *Inorg. Chem.* **1971**, *10*, 1559−1563.
(44) Morrison, W. H.; Hendrickson, D. N. *Inorg. Chem.* **1975**, *14*, 2331−2346.
(45) Kahn, O. *Molecular Magnetism*; VCH Publishers: New York, 1993.

found for solid-state molecular ferrocene. Moreover, the two shortest distances are similar in the two compounds: 5.673 versus 5.921 Å for two neighboring ferrocene moieties arranged edge-to-edge, from two neighboring layers, and 6.478 versus 6.494 Å for two neighboring ferrocene moieties arranged edge-to-face, from a single layer, for the title compound and the solid-state molecular ferrocene, respectively.[46] Ferrocene groups in $Zn(HO_3PFc)_2{\cdot}2H_2O$ present approximate D_{5h} symmetry since the cyclopentadienyl planes are almost parallel and eclipsed.

The thermal stability, limited to about 80 °C, shows the importance of the water molecules in the crystallographic arrangement. The drastic decrease in diffraction signal on heating at 140 °C illustrates the loss of the crystallographic arrangement within and between the chains. Nevertheless, the (020) reflection remains clearly observable evidencing that the ferrocene layer arrangement has not been lost yet. From this observation, along with the short C−H $-$ π distance around 3.7 Å within the ferrocene layers, one might infer that the ferrocene moieties arrangement is the driving force in the crystallographic organization, thus providing an organized assembly for the whole. Apart from the 2D arrangement of the ferrocene layers, the structure exhibits strong chemical bonding only along the *c* axis, producing the backbone of the structure and giving its 1D feature. Most metal phosphonates show layered arrangements, and only a few examples with linear arrangements have been reported on zirconium,[47] vanadium,[48,49] uranium,[50−52] molybdenum,[53] cadmium,[54] and iron[55] phosphonates. To our knowledge, no 1D zinc phosphonate have been obtained yet, but a linear zinc dimethyl phosphate[56] and ladderlike zinc phosphate[57] and zinc phosphonate[54] have been described with corner sharing of strictly alternating ZnO_4 and PO_4 tetrahedrons. Besides this, coordination polymers containing ferrocene are usually either ferrocene-substituted carboxylates or ferrocene-substituted pyridine, pyrimidine, or pyrazine.[58] Most of them adopt a low-dimensional crystallographic arrangement in the form of chains,[58−61] double-helix,[62] or dimers.[63] As in the title compound, all these inorganic polymers bear the ferrocene moiety on the side of the chain, as in our phosphonate, rather than within the chain itself.

The structural features suggest that the conductivity should be low, which is confirmed by the conductivity behavior. The values of σ_0 and E_a point to a mechanism driven by default according to the classification of Colomban and Novak and is close to the one observed for diamine-$\alpha Zr(HPO_4)_2$.[64]

The well- resolved central doublet observed by Mössbauer spectroscopy for the oxidized compound ($IS_{2b} = 0.432$ mm.s^{-1}, $QS_{2b} = 0.205$ mm.s^{-1}, $\Gamma_{2b} = 0.272$ mm.s^{-1}) is consistent with a stable S = 1/2 ferrocenium state as compared to the Mössbauer time scale (10^{-7} s). This S value leads for the effective moment to a spin only value of 1.73 μ_B; however, as commonly expected for S = 1/2 ferrocenium, anisotropy and a significant orbital contribution lead to a *g* value of 2.7, thus to a higher effective moment for S = 1/2 ferrocenium of 2.34 μ_B.[39,41,43] The corresponding *C* value is 0.68 emu.K.mol^{-1}. The same value was used in previous studies to determine the amount of intercalated ferrocene in α-$VOPO_4$.[40] The *C* value obtained for oxidized $Zn(HO_3PFc)_2{\cdot}2H_2O$ (**2**) is 0.268(1) emu.K.mol^{-1}, thus equivalent to an average value for **2** of 0.268/2 emu.K per mole of ferrocene. This result, along with the expected 0.68 emu.K.mol^{-1} for ferrocenium, leads to a ratio of oxidized ferrocene in $Zn(HO_3PFc)_2{\cdot}2H_2O$ of 20%. This value agrees very well with the 22.8(3.6)% obtained by Mössbauer signal fitting. Galvanostatic titration of the title compound has shown that it was possible to recover a maximum of 0.35 electrons per mole of ferrocene, that is, 35% of the ferrocene was reversibly oxidized. Taking into account the low conductivity of the sample, the oxidation process for the galvanostatic titration is thought to proceed by incorporation of ClO_4^- counteranions from the electrolyte rather than by migration of the cation out of the structure. Oxidation by iodine might also occur exclusively at the surface of the crystallites, without necessity of I_3^- migration within the crystallite, and where I^- can be located nearby the ferrocenium. The difference in the amount of oxidized iron between these two experiments may be explained by the difference between the processes used to achieve the oxidation. Moreover, the grain size could be slightly different between the experiments. Indeed, in the electrochemical measurements, the sample was finely ground and mixed with carbon black. In addition to the conductivity measurements, these results reinforce the idea of a surface-to-volume response. A calculated evaluation of the crystallite size which leads to 30% of the ferrocene moieties on the external surface of the crystallite leads to a reasonable value of 10 nm edge cubelike crystallite. Therefore, all reversible oxidation observed here could be due only to ferrocene moieties present on the surface of the crystallites.

Conclusion

We have presented a study of a peculiar hybrid solid, exhibiting a 1D arrangement along with 2D structural features. Its oxidation rate is limited by the lack of ionic conductivity. Nevertheless, the electrochemical response of the ferrocenylphosphonate synthon was efficient on a single surface scale, in such a manner that electrode modification for chemical sensors with these synthons might be considered. The functionalization of ferrocene by a phosphonate group might also be considered for use in optical and medical devices.

(46) Brock, C. P.; Fu, Y. *Acta Crystallogr., Sect. B: Struct. Sci.* **1997**, *B53*, 928−938.
(47) Zhang, B.; Poojary, D. M.; Clearfield, A. *Inorg. Chem.* **1998**, *37*, 249−254.
(48) Bonavia, G.; Haushalter, R. C.; Oconnor, C. J.; Zubieta, J. *Inorg. Chem.* **1996**, *35*, 5603−5612.
(49) Soghomonian, V.; Chen, Q.; Haushalter, R. C.; Zubieta, J. *Angew. Chem., Int. Ed. Engl.* **1995**, *34*, 223−226.
(50) Britel, A.; Wozniak, M.; Boivin, J. C.; Nowogrocki, G.; Thomas, D. *Acta Crystallogr., Sect. C: Cryst. Struct. Commun.* **1986**, *C42*, 1502−1505.
(51) Grohol, D.; Gingl, F.; Clearfield, A. *Inorg. Chem.* **1999**, *38*, 751−756.
(52) Grohol, D.; Subramanian, M. A.; Poojary, D. M.; Clearfield, A. *Inorg. Chem.* **1996**, *35*, 5264−5271.
(53) Poojary, D. M.; Zhang, Y.; Zhang, B.; Clearfield, A. *Chem. Mater.* **1995**, *7*, 822−827.
(54) Clearfield, A.; Sharma, C. V. K.; Zhang, B. *Chem. Mater.* **2001**, *13*, 3099−3112.
(55) Bujoli, B.; Palvadeau, P.; Rouxel, J. *Chem. Mater.* **1990**, *2*, 582−589.
(56) Harrisson, W. T. A.; Nenoff, T. M.; Gier, T. E.; Stucky, G. D. *J. Mater. Chem.* **1994**, *4*, 1111−1115.
(57) Wiebcke, M. *J. Mater. Chem.* **2002**, *12*, 421−425.
(58) Gang, L.; Hongwei, H.; Linke, L.; Xiangru, M.; Yaoting, F.; Yu, Z. *Inorg. Chem.* **2003**, *42*, 4995−5004.
(59) Hongwei, H.; Linke, L.; Gang, L.; Yaoting, F.; Yu, Z. *Inorg. Chem.* **2003**, *42*, 3501−3508.
(60) Horikoshi, R.; Ueda, M.; Mochida, T. *New J. Chem.* **2003**, *27*, 933−937.
(61) Dong, G.; Hong, M.; Chun-Ying, D.; Feng, L.; Qing-jin, M. *J. Chem. Soc., Dalton Trans.* **2002**, 2593−2594.
(62) Chen-jie, F.; Chun-ying, D.; Dong, G.; Cheng, H.; Qing-jin, M.; Zhe-ming, W.; Chun-hua, Y. *Chem. Commun.* **2001**, 2540−2541.
(63) Hongwei, H.; Gang, L.; Linke, L.; Yu, Z.; Xiangru, M.; Yaoting, F. *Inorg. Chem.* **2003**, *42*, 428−435.
(64) Colomban, P.; Novak, A. *J. Mol. Struct.* **1988**, *177*, 277−308.

Experimental Section

Synthesis. One hundred milligrams (0.38 mmol) of ferrocenylphosphonic acid was dissolved in 10 mL of water. This solution was adjusted to pH 4 and 430 mg (1.45 mmol) of $Zn(NO_3)_2 \cdot 6H_2O$ was added. The mixture was left at room temperature for five days. The solution was then filtered off and the precipitate washed with methanol and ether, and subsequently dried under vacuum. The resulting solid, $Zn(HO_3PFc)_2 \cdot 2H_2O$, contained numerous yellow needles (87 mg, 0.14 mmol, yield 73%). Elemental analysis calcd (%) for $ZnFe_2P_2O_8C_{20}H_{24}$ (631.5): Zn 10.35, Fe 17.67, P 9.82, C 38.00, H 3.80; found: Zn 10.27, Fe 17.28, P 9.32, C 37.94, H 3.76. IR (Nicolet AVATAR 320 FT, KBr pellet) (cm^{-1}): 3599(m), 3391(m), 3102(m), 2890(br), 2360(br), 1623(m), 1428(w), 1386(w), 1134(s), 1106(s), 1081(vs), 1054(s), 816(m), 483(m). ^{31}P MAS NMR (Bruker DPX 300, 121.5 MHz, ref H_3PO_4 30%) 22.7 ppm.

Crystallography. Data were recorded with an Xcalibur CCD camera (Oxford Diffraction) using graphite monochromated Mo Kα radiation ($\lambda = 0.71073$ Å) at 173 K, 40 s per frame. The structure was easily solved using direct methods[65] and refined using full-matrix least squares.[66] The final stages of the refinement were hampered because the data/parameter ratio was rather low, this being due to the small amount of scattering matter; all crystals formed as tiny needles with a diameter of typically 50 micron. To keep the data/parameter ratio to a reasonable value (10), it was decided to refine only the heavy atoms (Fe, Zn, and P) with anisotropic atomic displacement parameters. The hydrogen atoms of the cyclopentadienyl rings were placed geometrically. The hydrogen atoms of the hydroxyl group and the water molecule were hardly visible in the Fourier difference map, so that they are not too well placed with respect to their parent atoms. In addition, the presence of more peaks around the water molecule indicates that there is orientational disorder. Temperature-dependent powder X-ray diffraction data were collected on a Philips X'pert Pro diffractometer equipped with an X'Celerator detector and an Anton Paar HTK 1200 furnace and using CuKα radiation ($\lambda = 1.5418$ Å).

Thermogravimetric Analysis. Data were collected with a 2950 TGA HR V5.4A (TA Instruments) thermogravimetric analyzer, under nitrogen atmosphere, with a heat rate of 2 °C/ mn.

Conductivity. The material was equilibrated in a 60% RH atmosphere. Cylindrical pellets of 10-mm diameter and 1.95-mm thickness were prepared by cold pressing at 750 Mpa. The material was sandwiched between graphite electrode and placed into an airtight cell. Conductivity measurements were performed by the complex impedance method carried out with a frequency analyzer (Solartron 1174). The frequency range was from 1 to 10^6 Hz, and the temperature cycle was comprised between −20 and 85 °C. The stability is ±0.25 °C using the Pelletier effect. An "RKQ" (R and K in parallel with Q in series) model developped by Casciola and Bianchi was applied to simulate the impedance spectra.[33] After removal of the geometric capacitance of the cell, the impedance plots were refined by the expression: $Z = (R.Z_k/(R + Z_k)) + Z_Q$, where K and Q are constant phase angle elements related to dielectric relaxation in the material and electrode phenomena, respectively, and expressed as $Z_k = K^{-1}(j\omega)^{-n}$ and $Z_Q = Q^{-1}(j\omega)^{-p}$ ($0 \leq (n, p) \leq 1$).

Battery Preparation and Electrochemical Measurements. The active material was mixed with carbon black (Super S from Chemetals Inc., Baltimore, MD), 13 wt %, and PVDF binder, 6 wt %, to make a composite electrode on an aluminum disk. The electrodes had a surface area of 1 cm^2 and contained about 5 mg of active material. The electrolyte was a 1 M solution of $LiClO_4$ in propylene carbonate. Swagelok test cells were assembled in an argon-filled glovebox with moisture and oxygen levels less than 1 ppm. Li metal was used as anode. The batteries were tested using a VMP system (Claix, France) in a galvanostatic or potentiostatic mode. The coulometric titration (galvanosatic mode) is calculated from the elapsed time, the intensity, the active material mass, and the formula weight, according to the Faraday law and assuming that the experimental capacity during the reduction process is directly associated with the electrochemical response of the active material. The potential step was 10 mV/h.

Mössbauer Spectroscopy. ^{56}Fe Mössbauer spectra were recorded by transmission in the constant acceleration mode using an EG&G spectrometer. The sample was ground, mixed with grease, and then placed between aluminum sheets. Isomer shifts are given as referenced to high-purity α-Fe foil. The spectra were fitted to Lorentzien profiles by least-squares method using the ISO program.[67]

Magnetic Measurements. Data have been collected on an Oxford Instrument 9T VSM magnetometer. The powder was placed in a cellulose capsule. Data were corrected for the sample holder and the elements diamagnetic contributions.

Acknowledgment. We thank Dr. J-C. Jumas for recording the Mössbauer data, Dr. D. Ravot and C. Reibel for recording the magnetization data, Dr. R Astier and D. Granier for recording the crystallographic data.

Supporting Information Available: X-ray crystallographic data (CIF, PDF). This material is available free of charge via the Internet at http://pubs.acs.org.

JA049457P

(65) Altomare, A.; Burla, M. C.; Camalli, M.; Cascarano, G. L.; Giacovazzo, C.; Guagliardi, A.; Moliterni, A. G. G.; Polidori, G.; Spagna, R. *J. Appl. Crystallogr.* **1999**, *32*, 115−119.

(66) Watkin, D. J.; Prout, C. K.; Carruthers, J. R.; Betteridge, P. W.; Cooper, R. I. *CRYSTALS Issue 12*; Chemical Crystallography Laboratory: Oxford, U.K., 2001.

(67) Kündig, W. *Nucl. Instrum. Methods* **1979**, *75*, 336−340.